International Journal of Scientific Research in Engineering and Management (IJSREM)
Volume: 07 Issue: 03 | March - 2023 Impact Factor: 7.185 ISSN: 2582-3930

Mushroom like EBG to improve the Gain and Broadband of Patch Antenna for Ku-Band Satellite Application

DHARUGUPALLY VASAVI , GUNDETI DEEPAK

***Abstract*— In order to increase the gain of the patch antenna , a Mushroom-like EBG(Electromagnetic Band Gap) structure is used . EBG structures enhance the patch antenna's characteristics of directivity, bandwidth and efficiency . Initially, we determined frequency band gap characteristics of mushroom-like EBG unit cell value by using ANSYS software . The periodic arrangement of such mushroom-like EBG structure was not limited by any inter connecting microstrip lines . Different patches of similar configuration were arranged in a pattern to better improvement in an antenna performance . The final design shows an effective increase in Gain . The current distributions on those metal patches are nearly uniform, allowing for substantial gains throughout the working bandwidth.**

Keywords—EBG , mushroom-like EBG, ANSYS software ,Broadband .

1. INTRODUCTION

Microstrip patch antenna is mostly used due to its more advantages and better properties . They are lighter in weight , low volume , low cost , low profile , smaller in dimension and easy to fabricate .As we are concentrating on the gain improvement, additionally mushroom like EBG structure is used to increase the gain of antenna , decrease the back radiation and reducing in the size of antenna .Due to the compressed size of the high dielectric constant substrate with the microstrip antennas, they are exciting topic in its design .However, using this high dielectric constant substrate will cause major drawbacks like narrowing of bandwidth, inappropriate radiation patterns and decreased efficiency. To broaden the bandwidth of Microstrip patch antenna , variety of methods were employed, like increasing the thickness of substrate [1], Dividing the patch into slots[2], Introducing aperture coupling feeding network[3], Building shorting walls[4], Arranging parasitic strips around the patch[5],using hybrid-coupling method[6], and stacking patches on multilayered substrate[7].

In order to broaden the bandwidth of the Microstrip patch antenna, aforementioned methods are affective but they bring many other interesting aspects like size reduction, gain improvement, good radiation performances and planar structure.Recently, to achieve wideband performance, kinds of metamaterials were proposed. Among different kinds of metamaterials proposed, mushroom structure are most widely used in the design of broadband antennas.

One of the basic applications of mushroom structure is mushroom antennas.Because of the dual Resonance modes that were excited simultaneously, a low-profile mushroom antenna was presented in[8], and an impedance bandwidth of25% was obtained.

An impedance bandwidth from 56.3 to 65.7GHz was attained for a low-profile, low-temperature co-fired ceramic(LTCC)- based metamaterial mushroom antenna array fed by substrate integrated waveguide(SIW). An other promising application is loading mushroom-type structure on the conventional antennas. A new broadband antenna with bandwidths 4.5 to 5.6GHz was obtained by combining meta-mushroom structure and a software cavity-backed slot antenna[10]. A dual-band antenna is achieved for wireless local area network applications, after loading rectangular patch on the top of a planar slot[11]. As a result, after loading mushroom type metamaterial at SIE horn aperture, fractional impedance bandwidth of 10.6% was obtained on a $\lambda o/20$ thickness substrate[12]. Most of the Aforementioned antennas were constructed on multilayered substrate. On the basis of previous work[13], along with 2 radiating edges of a conventional path, a mushroom type structure is loaded on the same substrate. Conventional TM10 mode and a new quasi-TM30 mode are simultaneously excited, resulting in broad bandwidth

2. ANTENNA DESIGN

A. Antenna Geometry :

The suggested mushroom loaded patch antenna's geometrical configuration is shown in Fig. 1, and it consists of three parts: a main radiating patch, two parasitic mushroom-type arrays symmetrically positioned along the two radiating edges of the main radiating patch, and a ground plane with a size of lg x wg. The main radiating patch covers a distance of l w. An array of three mushroom-like structures are included in the mushroom-type structure. There are exactly the same number of mushroom units, and they are all the same size. A mushroom unit is made up of a square patch with periodicity p and a metallized via with diameter d in the centre. The coupling distance between the main radiating patch and mushroom-type structure is s, while the gap between mushroom units is g. This antenna uses a coaxial feeding method and is built on a substrate with a permittivity of 2.2, a loss tangent of 0.0009, and a thickness of 1.524 mm.

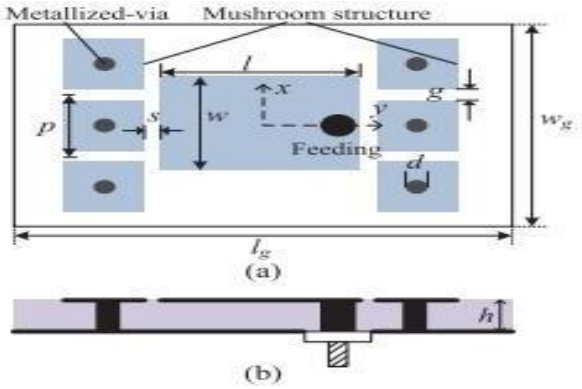

Fig. 1. Geometrical configuration of the proposed patch antenna. (a) Top view.
(b) Side view.

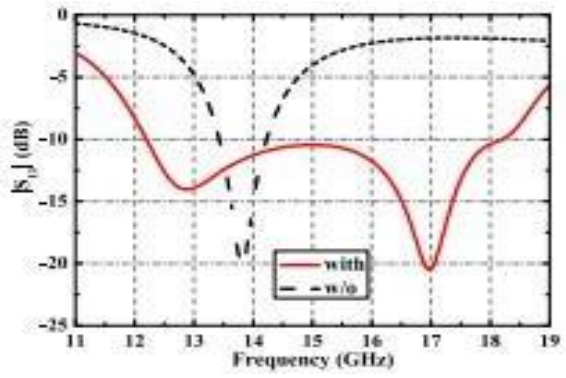

Fig. 2. Simulated |S11| of the patch antenna with and without the mushroom type structure.

B. Comparison with Conventional Patch Antenna

For comparison, a traditional patch antenna with the same size and feeding technique as the proposed antenna is presented. Because the mushroom-type structure is the only difference, Fig. 2 compares simulated |S11| of the patch antenna with and without the mushroom-type structure. Due of the loaded mushroomtype structure, a new resonance frequency is excited, resulting in a wide bandwidth of 12 to 18 GHz.

In order to intuitively illustrate the effectiveness of the loaded mushroom-type structure, the electric field distributions at two resonant frequencies are analysed. Figure 3 shows the simulated current and electric field distributions at the resonance frequency of 12.89 GHz. The electric field distribution is clearly identical to that of a conventional patch antenna in the TM10 mode. In fact, at low operating frequencies, the main radiating patch in the proposed antenna plays a vital role in radiating energy to free space. Because there is little energy passed to the mushroom-type structure in this scenario, the effect of a loaded mushroom-type structure can be ignored.

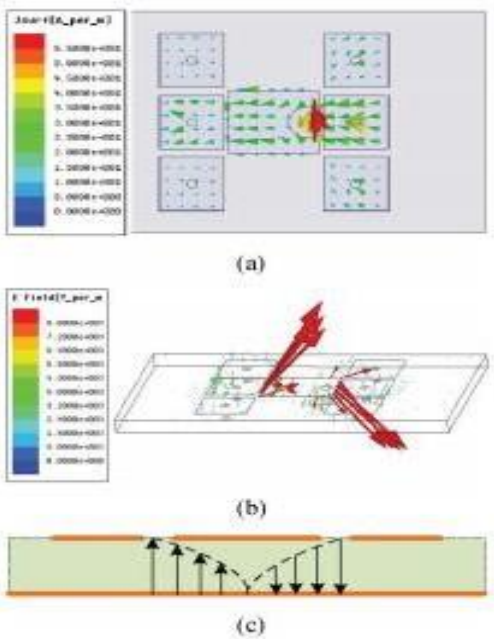

Fig. 3. TM10 mode at resonant frequency 12.89 GHz.

(a) Simulated current distribution.
(b) Simulated electric field distribution.
(c) Sketch of the operation mechanism.

At the new resonance frequency of 17 GHz, Fig. 4 shows the simulated current and

electric field distributions. The electric field distribution is found to be similar to the TM30 mode, specifically quasi-TM30 mode. Through coupling gaps, a portion of energy is coupled to the mushroom-like structure. As a result, energy can be radiated into space via two coupling gaps and two edges of a mushroom-like structure.

A transmission-line model is used to examine the suggested patch antenna in order to establish the resonance frequency for the quasiTM30 mode in theory. The extended length can be estimated to that of the matching whole rectangular patch, as shown in [10].

$$\varepsilon_{\text{eff}} = \frac{\varepsilon_r + 1}{2} + \frac{\varepsilon_r - 1}{2}\left(1 + 12\frac{h}{W_p}\right)^{-\frac{1}{2}} \quad (1)$$

$$\Delta L = 0.412h\frac{(\varepsilon_{\text{eff}} + 0.3)(W_p/h + 0.262)}{(\varepsilon_{\text{eff}} - 0.258)(W_p/h + 0.813)} \quad (2)$$

$$W_p = Np - g \quad (3)$$

$$\beta_e = k_0\sqrt{\varepsilon_{\text{eff}}} = \frac{2\pi f}{c}\sqrt{\varepsilon_{\text{eff}}} \quad (4)$$

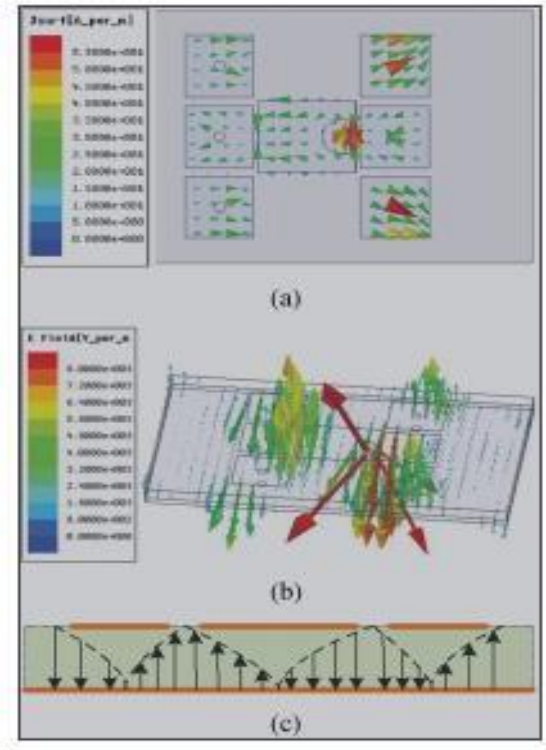

Fig. 4. Quasi-TM30 mode at resonant frequency 17 GHz.
(a) Simulated current distribution.
(b) Simulated electric field distribution.
(c) Sketch of the operation mechanism.

where eff is the substrate's effective dielectric constant, L is the extended length, Wp is the mushroom type structure's width, N is the number of mushroom units, and N in this letter equals 3. The propagation constant in the extended region is e, the free-space wave number is k0, the operational frequency is f, and the free-space velocity of light is c.

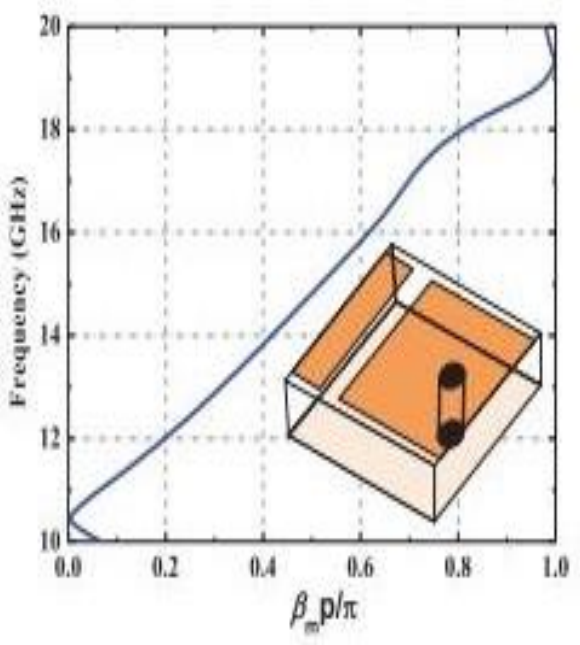

Fig. 5. Dispersion diagram of the mushroom unit.

The mushroom unit's propagation constant, m, can be calculated using the simulated dispersion diagram shown in Fig. 5. The proposed patch antenna is observed to be operated in the right-handed region. The quasiTM30 mode's resonance frequency is approximatively determined by

$$\beta_m pN/3 + 2\beta_e \Delta L = \pi. \qquad (5)$$

Overall, formula (5) may be used to calculate the resonant frequency for the quasi-TM30 mode, which is 17.9 GHz (where the corresponding mp/ is 0.794). Because the main driving patch has an effect on the resonant frequency, the computed frequency for the quasi-TM30 mode is slightly different from the simulated one of 17 GHz. Furthermore, two requirements must be met in order to efficiently excite quasi-TM30 mode: first, the number of mushroom units on one side must be odd, and second, the antenna construction must be symmetrical along the x- and y-axes.

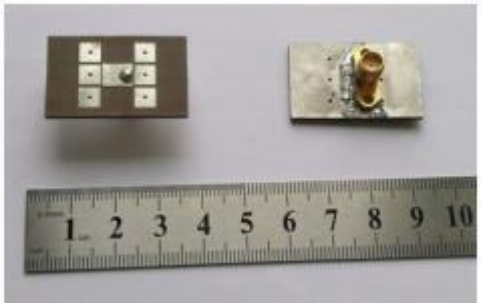

Fig. 6. Photograph of the proposed patch antenna.

Because the resonance frequency of the TM30 mode is about thrice that of the TM10 mode, wide bandwidth cannot be achieved by combining the TM10 and TM30 modes in a standard patch antenna. However, by loading mushroom type structure, the quasi-TM30 mode's resonance frequency approaches that of the TM10 mode, resulting in a large impedance bandwidth.

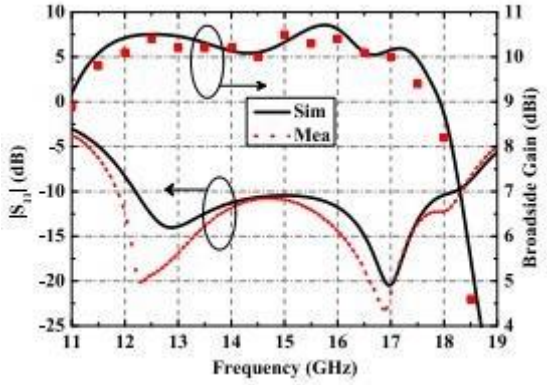

Fig. 7. Simulated and measured |S11| and broadside gains ofthe proposed antenna.

3. EXPERIMENTAL RESULTS

To validate the simulated results, a prototype of the suggested antenna is built and fabricated, as shown in Fig. 6. The following are the optimum parameters obtained by using the HFSS software to optimize the geometry of the mushroom-type loaded patch antenna: w = 5.6 mm, l = 6.9 mm

Num.	Impedance Bandwidth	0.5-dB Gain Bandwidth	3-dB Gain Bandwidth	Thickness	Number of Layers
[8]	34.9%	about 8.1%	about 30%	$0.08\lambda_0$	3
[10]	25%	about 7.6%	about 29%	$0.075\lambda_0$	2
[12]	22%	about 10%	about 30%	$0.08\lambda_0$	3
[14]	10.6%	about 3.5%	about 13%	$0.05\lambda_0$	1
This work	40%	34.5%	46%	$0.075\lambda_0$	1

mm, lg = 32 mm, wg = 20 mm, s = 0.3 mm, g = 0.7 mm, p =5.6 mm, d = 0.8 mm, h = 1.5 mm, s = 0.3 mm, g = 0.7 mm, p
= 5.6 mm, d = 0.8 mm, h = 1.5 mm The commercial SMA connector is placed along the y-axis with a 2.5 mm offset. Figure 7 shows the simulated and measured reflection coefficients and broadside gains. The results of the tests suggest that the proposed patch is effective.

The antenna operates with a |S11| of less than 10 dB from 11.9 to 18.2 GHz, which is more than 40% at the centre frequency of 15 GHz. The resonance frequencies that were measured were slightly shifted. downhill to a lower frequency, which could be caused by the manufacturing tolerance and dielectric loss Furthermore, the measured gains imply that the peak-radiating gain is almost constant The boresight direction yields between 10 and 10.5 dBi from 12 to 17 GHz. The proposed antenna's superiority of flat high gains makes it suitable for a wide range of applications.

Figure 8 depicts the simulated and measured far- field radiation patterns throughout the whole bandwidth at four typical frequencies. The simulated and measured results show a high level of agreement. The suggested antenna has been found to have stable broadside radiation patterns. Furthermore, because the cross polarization level in the E- plane is less than 40 dB, it is not visible in Fig. 8. In the H- plane, the measured amount of cross-polarization is lessthan 25 dB. Furthermore, the E-plane beam-widths are shorter than traditional patch antenna beam-widths, resulting in excellent gains. The quasi-TM30 mode dominates at high frequencies in the operational bandwidth, resulting in a high side-lobe level (SLL), as illustrated in Fig. 8's radiation pattern (h). The main radiation direction maintains broadside direction, but the gains are decreased rapidly because of the high SLL, which explains the sharply decreased gains after 18 GHz in Fig. 7.

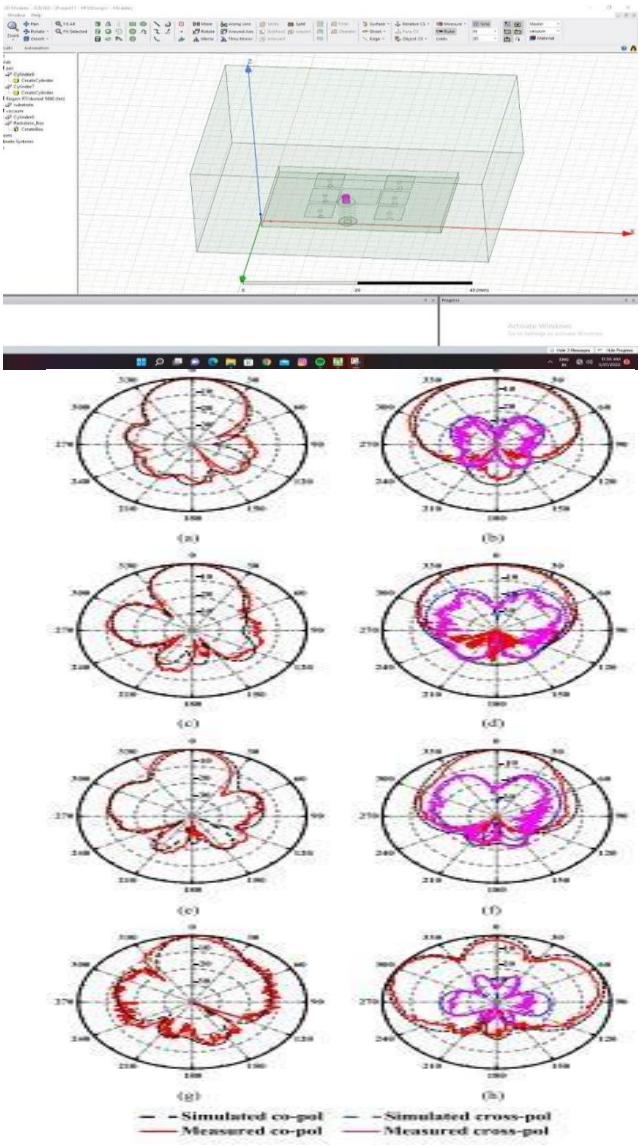

4. CONCLUSION

A unique broadband and high-gain microstrip patch antenna is researched in this letter. Because of the newly created quasi-TM30 mode, a wide impedance bandwidth characteristic is achieved by combining a mushroom-type structure with two radiating edges of a primary radiating patch. According to the results, an increased impedance bandwidth of more than 40% encompassing the whole Ku- band was achieved. Furthermore, the suggested antenna has constant broadside radiation patterns throughout the operating frequency range, with flat high gains about 10 dBi. Table I compares the structural parameters and performance of the proposed antenna with that of other previous antennas, indicating that the suggested antenna has the benefits of wide impedance bandwidth, high-gain flatness, low profile, and ease of fabrication.

5. REFERENCES

1) D. H.Schaubert, D. M. Pozar, and A. Adrian, "Effect of microstrip antenna substrate thickness and permittivity: Comparison of theories and experiment," *IEEE Trans.Antennas Propag*, vol. 37, no. 6, pp. 677–682, Jun. 1989.
2) A. A. Deshmukh and K. P. Ray, "Compact broadband slotted rectangular microstrip antenna," *IEEE Antennas Wireless Propag. Lett.*, vol. 8, pp. 1410–1413, 2009.
3) Y. Jia, Y. Liu, and S. Gong, "Slot-coupled broadband patch antenna," *Electron. Lett.*, vol. 51, no. 6, pp. 445–447, Mar. 2015.
4) Y. C. Chi, C. H. Chan, and K. M. Luk, "Study of a small wide-band patch antenna with double shorting walls," *IEEE Antennas Wireless Propag. Lett.*, vol. 3, pp. 230–231, 2004.
5) S. H. Wi, Y. S. Lee, and J. G. Yook, "Wideband microstrip patch antenna with U-shaped parasitic elements," *IEEE Trans. Antennas Propag.*, vol. 55, no. 4, pp. 1196–1199, Apr.2007.
6) K. P. Ray, G. Kumar, and H. C. Lodwal, "Hybrid-coupled broadband triangular microstrip antennas," *IEEE Trans. Antennas Propag.*, vol. 51, no. 1, pp. 139–141, Jan. 2003.
7) V. P. Sarin, M. S. Nishamol, D. Tony, C. K. Aanandan, P. Mohanan, and K.Vasudevan, "A wideband stacked offset microstrip antenna with improved gain and low cross polarization," *IEEE Trans. Antennas Propag.*, vol. 59, no. 4, pp. 1376–1379, Apr. 2011.
8) W. Liu, Z. N. Chen, and X. Qing, "Metamaterial-based low- profile broadband mushroom antenna," *IEEE Trans. Antennas Propag.*, vol. 62, no. 3, pp. 1165–1172, Mar. 2014.
9) W. Liu, Z. N. Chen, and X. Qing, "60-GHz thin broadband high-gain LTCC metamaterial-mushroom antenna array,"*IEEE Trans. Antennas Propag.*, vol. 62, no. 9, pp. 4592– 4601, Sep. 2014.
10) H.Kang and S. O. Park, "Mushroom metamaterial based substrate integrated waveguide cavity backed slot antenna with broadband and reduced back radiation," *Microw., Antennas Propag.*, vol. 10, no. 14, pp. 1598–1603, Nov. 2016.
11) Z. Wu, L. Li, X. Chen, and K. Li, "Dual-band antenna integrating with rectangular mushroom-like superstrate for WLAN applications," *IEEE Antennas Wireless Propag. Lett.*,vol. 15, pp. 1004–1007, 2016.
12) Y. Cai, Y. S. Zhang, L. Yang, Y. F. Cao, and Z. P. Qian, "Design of lowprofile metamaterials-loaded substrate integrated waveguide horn antenna and its array applications," *IEEE Trans. Antennas Propag.*, vol. 65, no. 7,pp. 3732–3737, Jul. 2017.
13) Y. Cao, Y. Zhang, Y. Cai, J. Zhang, and Z. Qian, "Wideband and high gain patch antenna loaded with mushroom-type metamaterial," in *Proc.Int.Conf. Microw.Millim. Wave Technol.*, May 2018, pp. 1–3.
14) K. F. Lee and K. F. Tong, "Microstrip patch antennas—Basic characteristics and some recent advances,"*Proc. IEEE*, vol. 100, no. 7, pp. 2169–2180, Jul. 2012.
15) Y. Dong and T. Itoh, "Metamaterial-based antennas," *Proc. IEEE*, vol. 100, no. 7, pp. 2271–2285, Jul. 2012.